J. Fluid Mech. (1992), *vol.* 234, *pp.* 669–690
Printed in Great Britain

On the applicability of various scaling laws to the turbulent wall jet

By I. WYGNANSKI, Y. KATZ AND E. HOREV
Department of Aerospace and Mechanical Engineering, University of Arizona, Tucson, AZ 85721, USA

(Received 12 June 1990 and in revised form 2 July 1991)

The spatial distribution of the mean velocity in a two-dimensional turbulent wall jet was measured for a variety of nozzle Reynolds numbers. It was determined that the bulk of the flow is self-similar and it depends on the momentum flux at the nozzle and on the viscosity and density of the fluid. The width of the nozzle which was commonly used to reduce these data has no part in the similarity considerations as has already been suggested by Narasimha *et al.* (1973). This type of self-similarity can be easily applied to determine the skin friction, which can otherwise only be determined with considerable difficulty. It was also shown that the 'law of the wall' applies only to the viscous sublayer. The Reynolds stress in the inviscid, inner portion of the flow is not constant thus the assumption of a 'constant stress layer' is not applicable. The applicability and universality of the 'outer scaling law' (i.e. Coles' law of the wake) has been verified throughout the inviscid inner portion of the wall jet. The logarithmic velocity distribution cannot be derived by making the usual assumptions based on the constancy of the Reynolds stresses or on the thinness of the logarithmic region relative to the thickness of the inner layer.

1. Introduction

Wall jets are mathematically described by the boundary-layer equations and are formally regarded as boundary-layer flows to which momentum was added upstream of the region of interest. Thus, the velocity somewhere in the boundary layer exceeds the velocity in the free stream. Wall jets are used in many diverse flow systems. For example, the flow over the external cowl of a fan-jet engine is a wall jet, as are the flows over an extended slotted flap of an airfoil and flow over the interior of an automobile wind shield when the defroster (or demister) is activated. Wall jets are used to shield turbine blades and other surfaces exposed to either hot or corrosive gases. Consequently, there are hundreds of reports describing various applications of a wall jet in industry.

A two-dimensional, turbulent and isothermal wall jet, flowing over a flat surface in the absence of an external stream is the prototypical configuration whose characteristics were investigated in most detail. The first experimental study of this flow, carried out by Forthmann (1934), was limited to measurements of mean velocities in the vicinity of the nozzle. Sigalla (1958), who tried to establish experimentally the skin friction in this flow, also measured the mean-velocity profiles at much larger distances from the nozzle than Forthmann. Numerous experimental investigations were carried out during the 1960s when the hot-wire anemometer came of age and statistical data of many turbulent shear flows were compiled. Most of the published data have been critically reviewed by Launder & Rodi (1981, 1983)

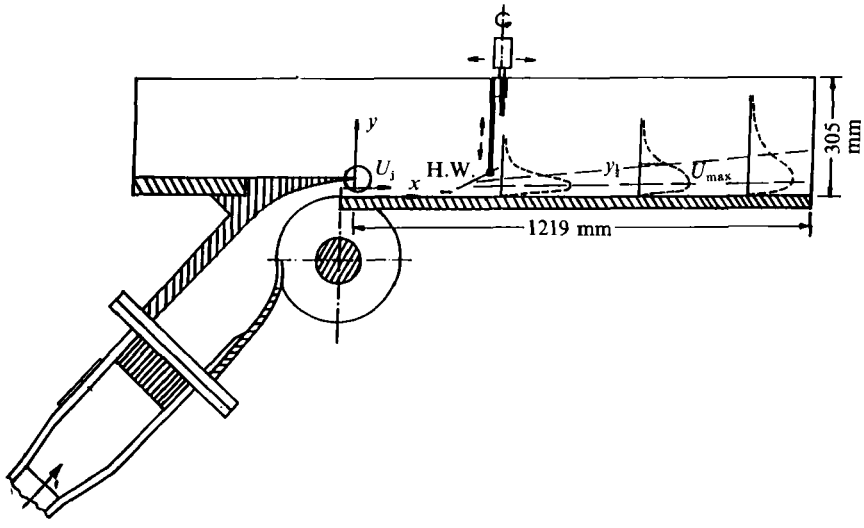

FIGURE 1. A schematic diagram of the apparatus.

and will not be repeated here; there are however a few endemic problems associated with this flow which should in our opinion be discussed.

For example, the rate of spread of the wall jet and decay of its maximum velocity in the direction of streaming appear to be dependent on the Reynolds number (Tailland & Mathieu 1967). Since such a dependence was not observed in a free jet at comparable Reynolds numbers one cannot help but wonder as to its origin. It is convenient to attribute this dependence to the presence of the solid surface but the latter contributes very little to the total momentum loss. In fact Narasimha, Narayan & Parthasarathy (1973) suggested that the traditional scaling of the relevant distances in the wall jet by the characteristic dimension of the nozzle might be erroneous. They proposed scaling the streamwise evolution of the flow by the momentum flux and the viscosity of the fluid, but their suggestions seems to have been ignored. Launder & Rodi (1981) discarded the novel scaling because many of the data sets used by Narasimha *et al.* were considered to have poor two-dimensionality.

Another vexing problem plaguing this flow stems from the difficulties encountered in measuring the wall shear stress. Some inconsistencies reported in the literature are attributed to the lack of two-dimensionality, to the thinness of the inner layer and to poor experimental techniques. Many devices commonly used to determine skin friction in turbulent boundary layers rely on the universality of the 'law of the wall', yet this universality has been repeatedly questioned in the case of the wall jet. A wide variety of log-law constants are quoted by some investigators (e.g. R. P. Patel 1962; Tailland & Mathieu 1967) while others (e.g. Ozarapoglu 1973; Irwin 1973) observe the universal constants for similar flow conditions. This controversy has practical implications since the number of engineering tools used to estimate surface friction would be greatly reduced if the universal law does not apply to the wall jet.

The universality of *outer scaling* analogous to 'the law of the wake' (Coles 1956) was never tested in the wall jet, perhaps because of the original name. Coles (1956, p. 196), however, viewed the universality of the law of the wake as a manifestation of the large-scale mixing process which is constrained by inertia rather than by viscosity. Wherever such flow is bounded by a wall, it is further constrained by the

no-slip condition at the solid surface. The inner and outer scaling laws should thus overlap in some region of the flow. The inner portion of the turbulent wall jet fulfils the same physical criteria in spite of the fact that the total momentum in the outer flow is finite.

The present investigation of the wall jet was undertaken in order to assess the relevance of the solid surface to the evolution of the large coherent structures in otherwise inviscidly unstable flow. From this point of view the wall jet resembles a boundary layer in a strong adverse pressure gradient. We intend to subject the wall jet to external excitation and to observe its response. Before doing so however, the scaling laws governing the basic flow have to be identified and understood. The purpose of the present report is to focus on the unresolved and controversial issues in the unforced case.

The experiments were carried out in air, on the simplest wall jet configuration in the absence of an external stream or surface curvature. The flow was incompressible and the Reynolds numbers based on the efflux velocity and on the nozzle dimension ranged between 3×10^3 and 3×10^4. The variation in Reynolds numbers was achieved by changing the nozzle dimension as well as the efflux velocity.

2. Description of the experimental apparatus

A schematic diagram of the wall jet facility is shown in figure 1. The wall jet originated from a two-dimensional nozzle of an adjustable width not exceeding 10 mm and a span of 600 mm. The air flow for the jet was supplied by a centrifugal blower manufactured by North American Co. equipped with a Toshiba [model VF pack P1] speed controller which provided a very stable source of air. Filters were mounted at the inlet to the blower to protect the hot wires used to measure the velocity. A flexible hose connected the outlet of the blower to a diffuser and a settling chamber. The diffuser was equipped with a perforated plate and the settling chamber with an array of 4 screens in order to distribute the flow evenly and to reduce the turbulence level at the nozzle exit. The contraction ratio of the nozzle was variable as it depended on the preselected dimension of the slot. The nozzle was made from two eccentric circular arcs. The lower part of the nozzle was made from a solid, circular cylinder in which two notches were milled: one provided an anchor for the flat surface which constituted the wall of the wall jet while the other supported a thin metal membrane connecting the nozzle to the settling chamber. This cylinder was supported by screws pushing against a central shaft which protruded through a groove in the sidewalls of the apparatus. The width of the nozzle was altered by adjusting these screws and later levelling the 125 cm long flat plate at the downstream end of the facility.

The upper lip of the nozzle was fairly sharp and it had to be reinforced by a thicker plate equipped with adjustable screw jacks. The plate was located sufficiently far upstream of the lip so that it did not interfere with the entrained flow which was attached to the outer surface of the upper lip. The jet emerged from the nozzle with a top-hat velocity profile, with the exception of two thin boundary layers, one near the outer lip of the nozzle and one near the wall. The two-dimensionality of the jet was tested by traversing a small and flat total-impact tube across 90% of the span of the apparatus. Initial traverses were made at a constant distance, Y, from the surface of the wall at a streamwise distance of 10 slot widths downstream of the nozzle. The screw jacks in the reinforcing plate were adjusted during these traverses until the flow appeared to be two-dimensional. The uniformity of the slot width was

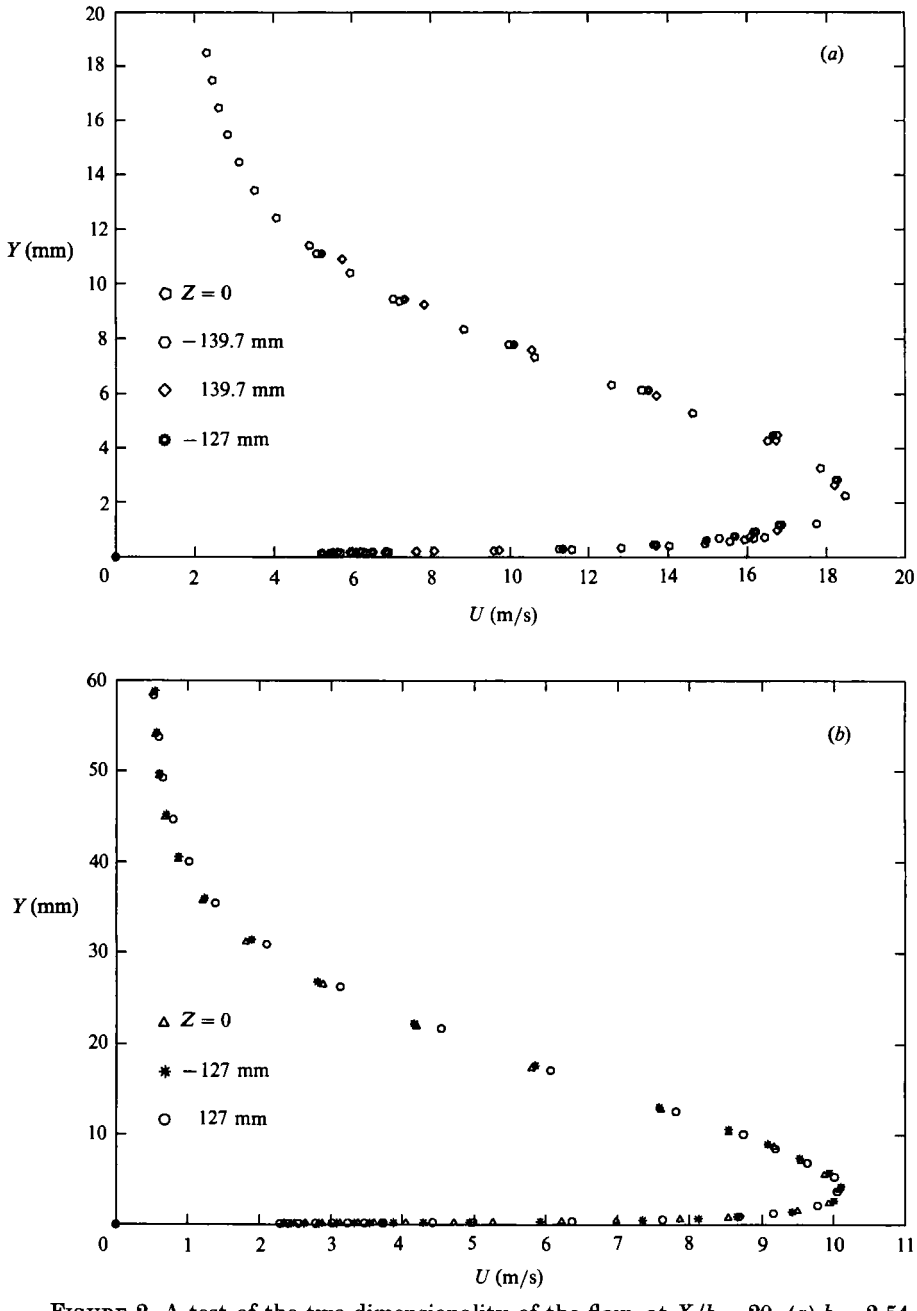

FIGURE 2. A test of the two-dimensionality of the flow, at $X/b = 20$. (*a*) $b = 2.54$ mm, $U_j = 30$ m/s, (*b*) $b = 7.62$ mm, $U_j = 15$ m/s.

continuously monitored during these adjustments. The final test of the two-dimensionality of the flow was made by traversing the wall jet at 3 to 4 spanwise locations, 20 slot widths downstream of the nozzle (figure 2).

The streamwise component of the velocity was measured in the self-similar region of the wall jet starting some 20 slot widths downstream of the nozzle. Most of the measurements extended beyond 100 slot widths from the nozzle where the maximum

velocity in the wall jet dropped to approximately one quarter of its initial value. The Reynolds number at the nozzle was altered by changing the efflux velocity, U_j, between 10 and 50 m/s and/or by changing the width of the slot, b, between 2.5 and 7.5 mm. The range of Reynolds numbers considered was: $3 \times 10^3 \leqslant Re_j \leqslant 3 \times 10^4$, where $Re_j \equiv U_j b/\nu$.

The streamwise component of velocity was measured with a single, boundary-layer-type, hot-wire sensor manufactured by Dantec (model 55P15) with a multi-channel anemometer manufactured by AA Lab Systems. The wire was calibrated at the nozzle exit for the range of velocities anticipated at the traverse location. The entire calibration procedure was done under computer control using a Baratron (model 170M) pressure transducer as reference. A fourth-order polynomial expression was used in order to linearize the hot-wire signal. The traverse mechanism was manual in the X- and Z-coordinates but it was driven under computer control by a stepper motor in the Y-coordinate. The velocity near the solid surface was measured at ΔY intervals of 0.01 mm.

Hot-wire data were acquired and analysed digitally. The hot-wire signal was conditioned by passing it through a buck-and-gain amplifier and a filter, both of which constituted an integral part of the AA Electronics anemometer unit. It was then digitized with a 12 bit resolution on a Masscomp computer.

3. Results

3.1. *Mean velocity and thickness*

Two out of six measured sets of normalized mean velocity profiles are plotted in figure 3. These two sets were chosen because the difference between them was the largest observed. Each set represents a superposition of eight individual profiles measured at distances ranging from 30 to 140 slot widths from the nozzle for a given nozzle Reynolds number Re_j. The velocity at each X-location was divided by its local maximum velocity U_m. The differences observed between the two sets of data may be attributed to the effect of Re_j. The nozzle Reynolds number might therefore have a slight effect on the dimensionless velocity profile at the outer part of the jet (i.e. at $Y/Y_{m/2} > 1.3$ where $Y_{m/2}$ is the distance measured from the wall to the location at which the mean velocity decreases to $\frac{1}{2}$ of its local maximum value in the outer part of the flow). However, the data taken in this region are not very reliable because of the possible presence of room draughts which may affect the measurements as well as the entrained flow. In fact, most of the previous measurements taken in the absence of an external stream terminate at $Y/Y_{m/2} = 1.6$ and there is a fair amount of scatter reported in the literature for $Y/Y_{m/2} > 1.3$. The velocity profile measured at $Re_j = 19000$ agrees very well with the velocity profile measured by Tailland & Mathieu (1967) at comparable Re_j. The latter is also plotted on figure 3 for visual comparison. One may conclude that the mean velocity distribution in the wall jet is self-similar and almost independent of Reynolds number, when it is normalized by the local length and velocity scales.

The decay of the maximum velocity in the jet with increasing distance from the nozzle is plotted in figure 4. Traditionally, the ratio of $(U_j/U_m)^2$ is plotted *vs.* X/b in order to accentuate the decay of the velocity scale which is expected to vary approximately as $1/X^{\frac{1}{2}}$. In this plot the streamwise distance is measured from a virtual origin X_o by requiring that the lines fitted through the data converge to $U_m/U_j = 1$ at $X = X_o$. (There is a somewhat irregular tendency of the virtual origin to move upstream with increasing Re_j. A notable shift in this origin occurred around

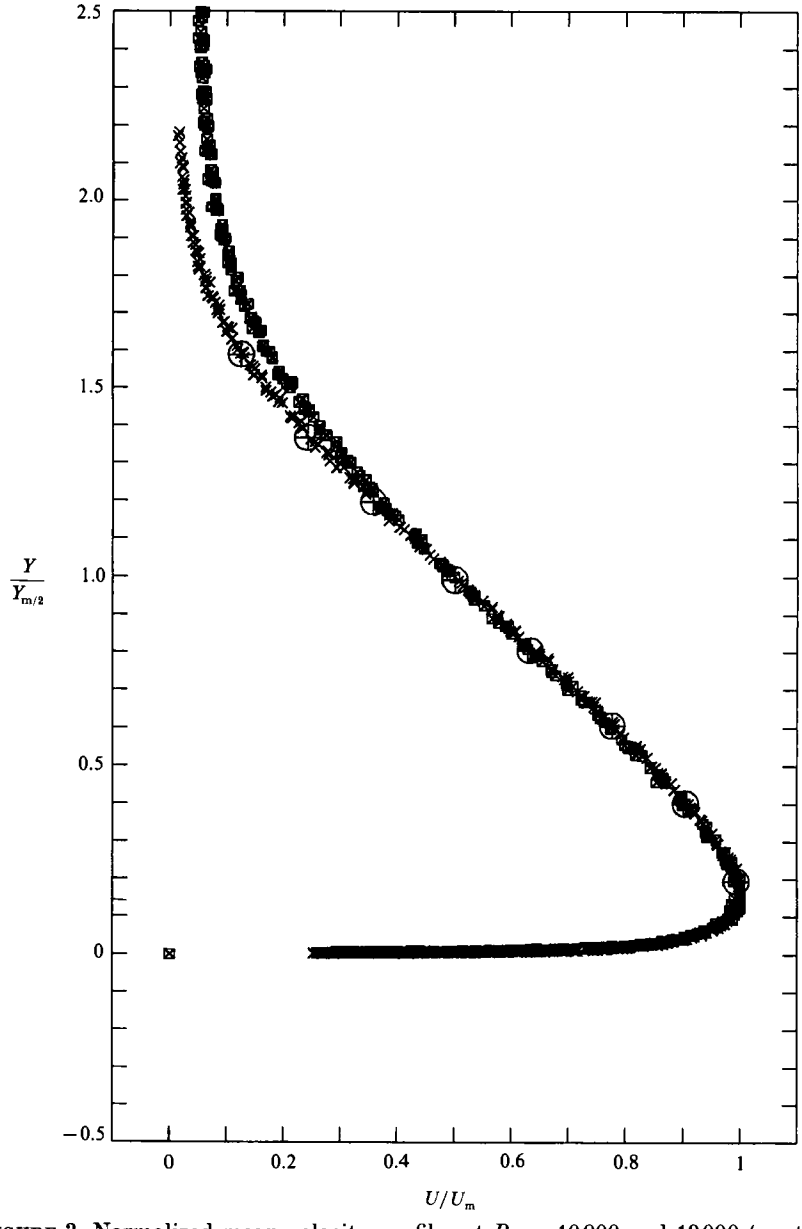

FIGURE 3. Normalized mean velocity profiles at $Re_j = 10000$ and 19000 (see table 1 for symbols), and compared to data from Tailland & Mathieu (1967) at $Re_j = 18000$.

$Re_j = 5000$ whereupon turbulence was first noticed near the solid surface in the plane of the nozzle. Near the upper lip of the nozzle the flow is oscillatory as a result of the Kelvin–Helmholtz instability so typical of a free mixing layer. The interaction between the flow oscillations near the wall and near the outer lip of the nozzle might be responsible for the complex dependence of X_0 on Re_j.) Straight lines represent the results plotted in figure 4 fairly well, but a power-law expression of the form

$$\left[\frac{U_m}{U_j}\right] = A_u\left[\frac{X-X_0}{b}\right]^n \tag{1}$$

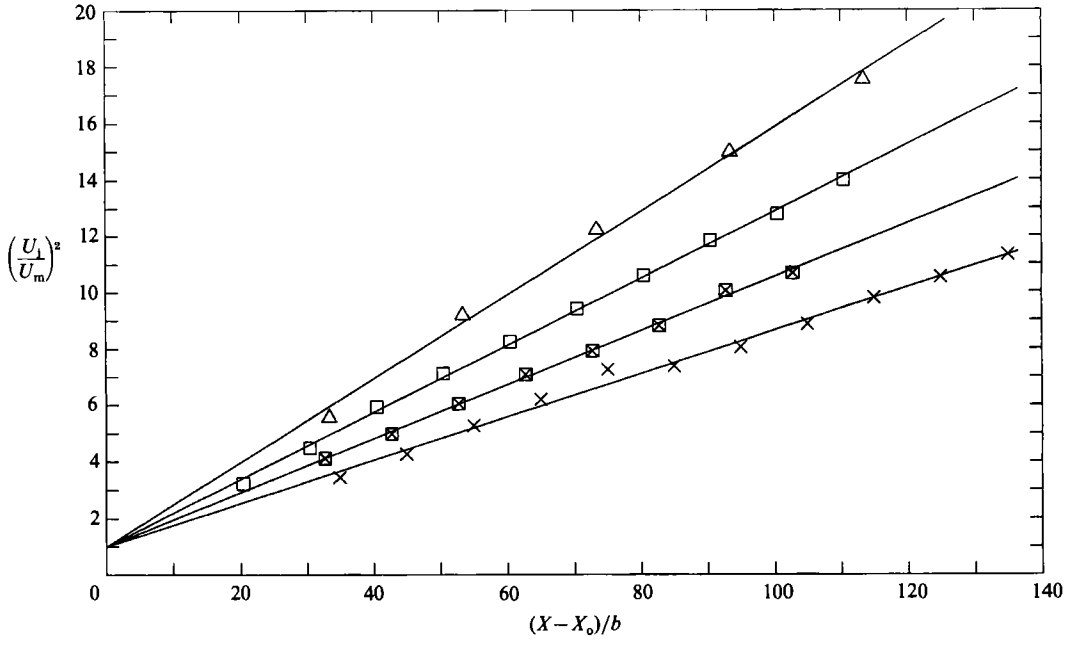

FIGURE 4. The decay of the maximum velocity in the jet as a function of downstream distance (or various Re_j values (see table 1).

Symbol	U_j (m/s)	b (m)	Re_j
×	57	5	19000
⬡	30	7.5	15000
⊠	30	5	10000
○, ▯	15	7.5	7500
□	15	5	5000
◇	30	2.5	5000
◁, △	10	5	3700

TABLE 1. Symbols used in figures

fits the data better when the exponent n is approximately -0.47. The corresponding exponent for the rate of spread of $Y_{m/2}$ with X is close to 0.88, in substantial agreement with the results of Narasimha *et al.* (1973), who suggested that this exponent should be 0.91. Nevertheless, Launder & Rodi (1981, 1983) preferred a linear relationship to describe the rate of spread of the flow and proposed the following relationship:

$$\frac{dY_{m/2}}{dX} = 0.073 \pm 0.002. \tag{2}$$

The effect of Reynolds number on the decay of the maximum velocity and the rate of spread of the jet in the present investigation is significant. In fact the slope of the lines drawn in figure 4 changes by a factor of 2 in the range of Re_j considered. Narasimha *et al.* (1973) suggested that the fully developed wall jet should attain a local equilibrium independent of the detailed conditions at the nozzle. The sole parameter determining the evolution of an incompressible wall jet surrounded by an

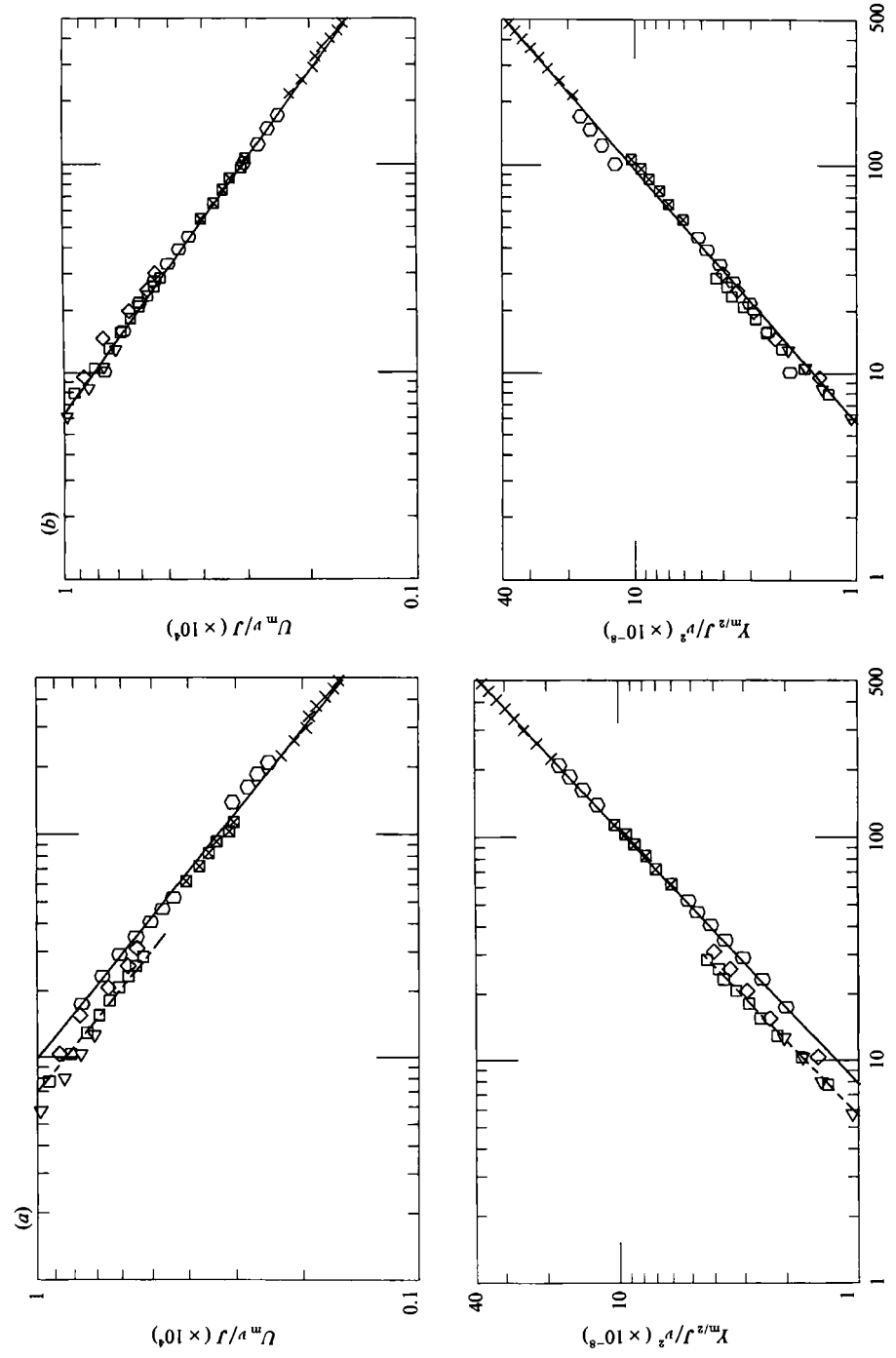

FIGURE 5. The dependence of the velocity and lengthscales on $\xi = XJ/\nu^2$. (*a*) The downstream distance is measured from the nozzle; (*b*) the downstream distance is measured from the virtual origin. For symbols see table 1.

identical fluid should therefore be the initial, kinematic momentum flux, J. This is conceptually identical to the scaling laws proposed for jets by Newman (1961) and for small-deficit wakes by Sreenivasan & Narasimha (1982). (Unfortunately the streamwise evolution of wakes is not entirely dependent on the drag of the body, or the momentum deficit in the flow as the previous authors had anticipated, because of a persistent dependence of the flow on the nature of the initial instability. Nevertheless, scaling the wakes by the momentum thickness is much more relevant than scaling by the typical body dimension (e.g. a diameter of a cylinder) which was traditionally used for this purpose.) Using Narasimha's suggestion one gets

$$\frac{U_m \nu}{J} = F_1(\xi); \quad \frac{Y_{m/2} J}{\nu^2} = F_2(\xi); \quad \tau_w/\rho\left(\frac{\nu}{J}\right)^2 = F_3(\xi), \tag{3}$$

where $\xi = [XJ/\nu^2]$, $J = [U_j^2 b]$, ρ and ν are the density and kinematic viscosity of the fluid respectively, τ_w is the shear stress at the wall and X is measured from the nozzle.

The velocity and the length scales plotted in this fashion prove the validity of Narasimha's assumptions and indicate that the flow is indeed independent of Re_j provided that the latter exceeds a threshold value of 5000 (figure 5*a*). The various values of Re_j shown in figure 5 were obtained by changing the slot width between 2.5 and 7.5 mm, or by changing the velocity between 10 and 57 m/s. The solid lines drawn through the high-Re_j data can be expressed analytically by the following power laws:

$$\left[U_m \frac{\nu}{J}\right] = A_u \left[X \frac{J}{\nu^2}\right]^n, \quad \left[Y_{m/2} \frac{J}{\nu^2}\right] = A_y \left[X \frac{J}{\nu^2}\right]^m, \tag{4a}$$

where $A_u = 1.473$; $n = -0.472$; and $A_y = 1.445$; $m = 0.881$.

Even for $Re_j \leqslant 5000$ the exponent representing the decay of the velocity scale or the rate of growth of the length scale with ξ remains unaltered, only the constant coefficient changes. The exponents suggested above compare quite favourably with the exponents recommended by Narasimha *et al.* ($m = 0.91$, $n = -0.506$) in spite of the fact that Narasimha established his proposed fit on the basis of data acquired at much larger ξ and Re_j. The constants A_u and A_y recommended by Narasimha are different but there is sufficient scatter in the original data collected in that article to account for the difference.

One may recast these data by accounting for the virtual origin as defined earlier (figure 5*b*) and completely eliminate the dependence of the length and velocity scales on Re_j:

$$\left[U_m \frac{\nu}{J}\right] = A_u \left[(X - X_0) \frac{J}{\nu^2}\right]^n, \quad \left[Y_{m/2} \frac{J}{\nu^2}\right] = A_y \left[(X - X_0) \frac{J}{\nu^2}\right]^m, \tag{4b}$$

where $A_u = 0.557$; $n = -0.428$; and $A_y = 9.246$; $m = 0.804$. The determination of the constants A_u and A_y is strongly dependent on the choice of the respective exponents n and m. Both plots are shown in figure 5 because they will be used in calculating τ_w and determining the consistency of the data.

3.2. *Turbulent fluctuations*

The cross-stream distribution of the streamwise component of the turbulent intensity does not even scale with $Y_{m/2}$ and U_m for the data acquired at a single Re_j let alone for a variety of Reynolds numbers. The data plotted in figure 6 were acquired at $Re_j = 5 \times 10^4$ and 19×10^4 at distances ranging from 60 to 120 slot widths downstream of the nozzle where the mean velocity profiles appear to be self-similar.

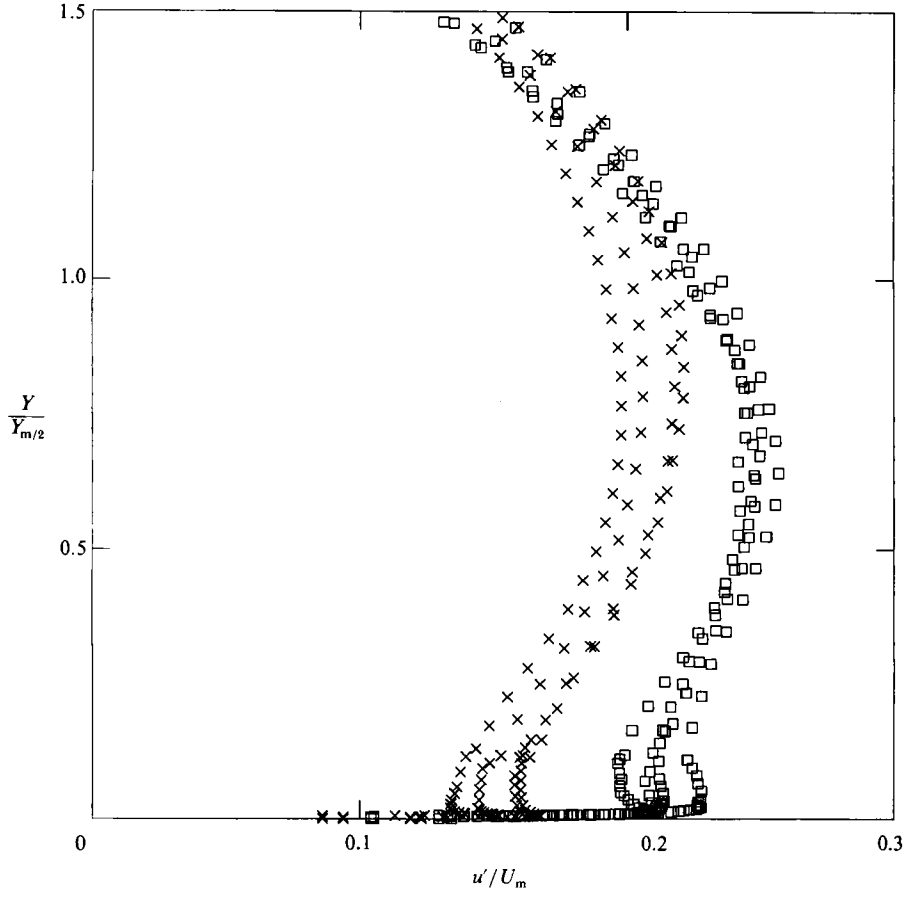

FIGURE 6. The distribution of u'/U_m across the jet. For symbols see table 1.

One might always argue that a distance of 100 slot widths is insufficient to attain similarity and to such an argument we cannot reply. It may be pointed out however, that in a free jet, self-similarity of all three components of the turbulent intensity is attained at much shorter distances from the nozzle. We therefore suspect that there exists a genuine lack of equilibrium caused by the viscous friction with the wall. The dependence of u'/U_m on X (where u' is the r.m.s. velocity) at the outer part of this flow (i.e. at $Y \gg Y_m$ which is generally assumed to behave like a free jet) implies that the wall inhibits the evolution of the large eddies well beyond the location at which $U = U_m$. The largest deviations from self-similarity are visible near the solid surface where the production of turbulent energy is highest, and no benefit was derived by replotting the data in wall coordinates (after establishing the friction velocity).

The lack of similarity exhibited by u'/U_m prompted us to re-examine the velocity distribution in the vicinity of the wall by replotting the data on a larger scale in figure 7 for two values of Re_j. It appears that the normalized velocity profile near the surface is weakly dependent on Re_j (regardless of any shift in the virtual origin) particularly when the latter is lower than 5000. The self-similarity near the wall is thus limited to the variation of the velocity profile with X at a prescribed Re_j. Although the deviation from similarity is small enough to not be observed in figure 3, it is large enough to indicate that the inner portion of the wall jet might not be self-similar because of the presence of the wall.

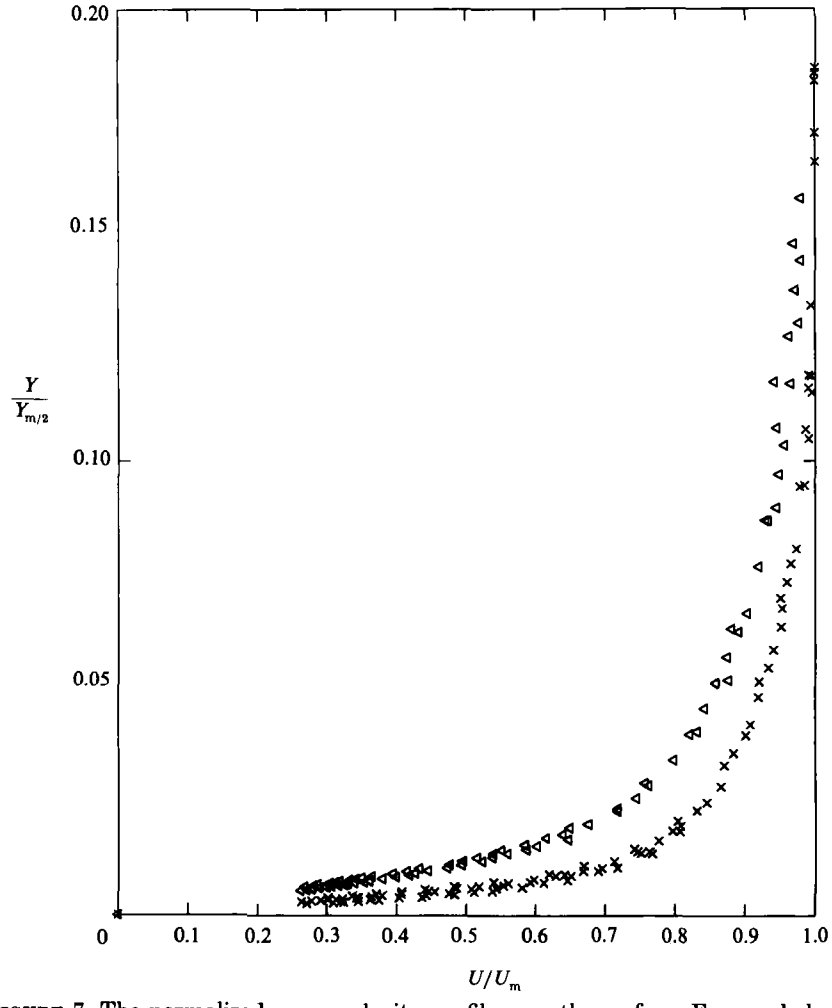

FIGURE 7. The normalized mean velocity profile near the surface. For symbols see table 1.

It is observed that the maximum velocity in the jet occurs at $Y/Y_{m/2} \approx 0.15$ which agrees very well with most of the results reported in the literature (see Launder & Rodi 1981, table 1). Since previous data were accumulated over a large range of Reynolds numbers and flow conditions – the results of Guitton & Newman (1977) on curved surfaces, and of Irwin (1973), in the simultaneous presence of a free stream and pressure gradient may also be included in this correlation – we may surmize that the ratio $Y_m/Y_{m/2}$ is insensitive to the details of the flow. Consequently one may consider $Y_{m/2}$ as the primary length by which the turbulent portion of the wall jet (i.e. the fraction of the flow which is dominated by Reynolds stresses) might be scaled. The separate tabulation of the external width of the flow measured from the location of the maximum velocity $Y_{m/2} - Y_m$ (e.g. Tailland & Mathieu 1967) seems to be superfluous.

3.3. *Wall shear-stress*

The determination of wall shear stress in this flow is very difficult because of the thinness of the inner boundary layer which extends from the surface to the location at which the jet velocity has a local maximum (i.e. where $Y \leqslant Y_m$). Since the wall

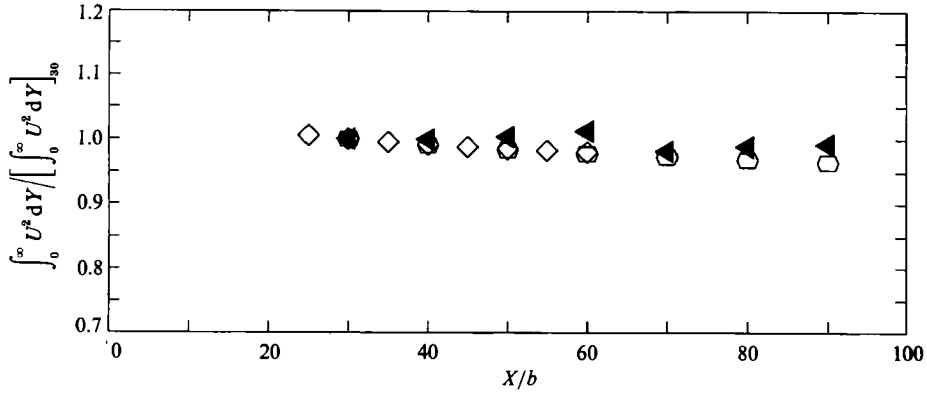

FIGURE 8. The decay of the jet momentum with downstream distance. Three methods are compared: ○, estimates from wall shear; ◇, Preston tube measurements; ◀, the use of integral momentum equation.

friction has little or no influence on the spreading of the flow, attempts to correlate the wall stress with the depreciation of the momentum integral in the direction of streaming were not very successful (e.g. Schwarz & Cosart 1961). The skin friction in previous experiments was either measured directly by using a small, floating drag balance or indirectly by calibrated surface heat-transfer devices or impact probes like the Stanton or Preston tubes (Launder & Rodi 1981; Ozarapoglu 1973). Since these devices are usually calibrated in channel flows they depend on the universality of the velocity profile and cannot extend in Y beyond the range in which the universal velocity distribution associated with the law of the wall applies.

The mean velocity gradient in the viscous sublayer, which has to be constant near the surface, can also be used to estimate the skin friction. This method, which was first used in the wall jet by Tailland & Mathieu (1967), was criticized by Launder & Rodi (1981) as being inaccurate because the estimates of C_f based on this technique 'have produced values ranging from 20% to 35% below the consensus values of impact tube data'. In the present experiment the shear stress at the wall was estimated by use of the momentum integral method, the mean velocity gradient in the viscous sublayer, and by use of a Preston tube. The latter method was only used in those cases where it was established (by using the first two methods) that the mean velocity profile expressed in the law-of-the-wall coordinates complies with the constants used for calibrating the tube.

The depreciation of the jet momentum in the direction of streaming for $Re_j = 5000$ is plotted in figure 8. The data were normalized by the jet momentum measured at $X/b = 30$. The frictional losses estimated from $[\mathrm{d}U/\mathrm{d}Y]_w$ were checked against the losses estimated from the momentum integral equation at $X/b = 30$ and 90. There is reasonably good agreement between the two methods. An independent check was provided by using a calibrated Preston tube based on the design of V. C. Patel (1965) for $Re_j = 5000$, since here the universal constants of the law of the wall based on the friction velocity, $U_\tau = (\tau_w/\rho)^{\frac{1}{2}}$ measured by the other techniques were actually realized (i.e. $U/U_\tau = 5.5 \log (YU_\tau/\nu) + 5.5$). The diameter of the Preston tube used in this experiment was 0.89 mm, corresponding to $14 < U_\tau d/\nu < 28$. one may therefore apply V. C. Patel's calibration curve (Patel 1965, p. 192). The result of these measurements confirmed that the momentum loss was estimated correctly by the other indirect means, thus justifying their use.

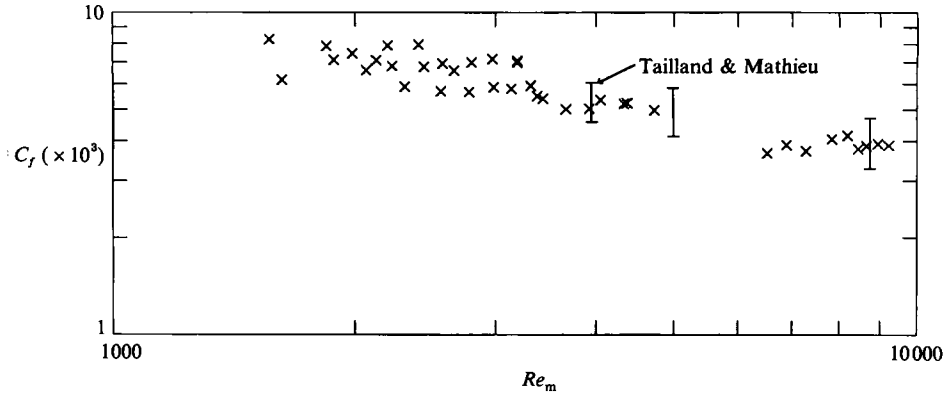

FIGURE 9. The dependence of C_f on the local Reynolds number (Re_m) and a comparison of the present results with those of Tailland & Mathieu (1967).

A plot of the dimensionless skin friction coefficient

$$C_f = \frac{\tau_w/\rho}{\frac{1}{2}U_m^2}$$

versus the local Reynolds number ($U_m Y_m/\nu$) is given in figure 9 and compared with the results of Tailland & Mathieu. The agreement between these two sets of data is good. Since the present results are entirely self-consistent, they cast some doubt on most of the impact-tube data reported in the literature which yield a much higher value of C_f.

We have decided that the most reliable method for measuring the wall stress is to use the slope of the mean velocity profile near the surface. We realized that the reliability of this method depends on the quality of the traversing mechanism used (a resolution of 0.01 mm might be required), the quality and size of the hot-wire probe and the number of data points taken to establish the slope correctly. Furthermore, heat loss from the wire to the surface may change the apparent slope of the velocity profile measured very close to the wall (Wills 1962), consequently such change in slope served as an indication for stopping the traverse. The data used for assessing the wall friction were taken at elevations exceeding 50 wire diameters above the surface and Reynolds numbers based on the wire diameter in excess of 0.7. The linear fit to the data extended in some cases to 100 wire diameters and Reynolds numbers of 1.5. For this range of variables the heat loss to the wall is not significant even in laminar flow, and less significant in turbulent flow (where the corrections suggested by Wills are approximately halved).

A plot of $(\tau_w/\rho)(\nu/J)^2$ versus ξ is presented in figure 10(*a*) where all the data obtained through the use of the adopted method are plotted in the general similarity coordinates. Once again the skin friction scales correctly with ξ and is independent of Re_j. The best fit to the data is given by

$$\frac{\tau_w}{\rho}\left(\frac{\nu}{J}\right)^2 = A_\tau \xi^k, \tag{5}$$

where $A_\tau = 0.146$ and $k = -1.07$.

A cross-check on A_τ and k can be obtained by assuming that the mean velocity is self-similar, giving

$$\int_0^\infty U^2 \,\mathrm{d}Y = \kappa U_m^2 Y_{m/2},$$

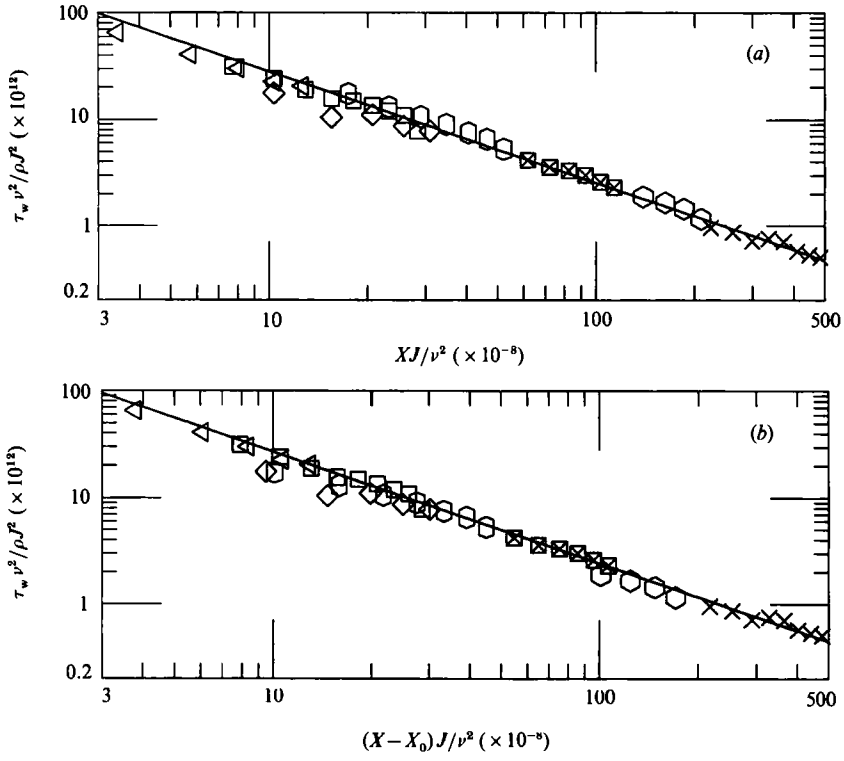

FIGURE 10. The variation of wall stress with $\xi = XJ/\nu^2$. (*a*) The downstream distance is measured from the nozzle, (*b*) the downstream distance is measured from the virtual original. For symbols see table 1.

where
$$\kappa = \int_0^\infty \left[\frac{U}{U_m}\right]^2 \mathrm{d}\left(\frac{Y}{Y_{m/2}}\right) = 0.74.$$

Then by using the momentum integral equation in conjunction with (4),

$$\frac{\tau_w}{\rho} = -\frac{\mathrm{d}}{\mathrm{d}X}\int_0^\infty U^2\,\mathrm{d}Y = -\kappa\frac{\mathrm{d}}{\mathrm{d}X}[U_m^2 Y_{m/2}]. \tag{6}$$

The exponent k is given by

$$k = 2n+m-1 = 2(-0.472)+0.881-1 = -1.063,$$

and the constant coefficient is

$$A_\tau = -\kappa(2n+m)A_u^2 A_y = 0.146.$$

One may also calculate k and A_τ from the data plotted in figure 5(*b*) which account for the virtual origin of the jet. In this case $k = -1.052$ and $A_\tau = 0.11$ which compares with the measured values of $k = -1.056$ and $A_\tau = 0.084$ obtained from figure 10(*b*).

The agreement between the measured shear stress at the wall and the calculated shear stress on the basis of flow similarity is good and thus may provide an alternative indirect method for estimating wall friction in a two-dimensional wall jet.

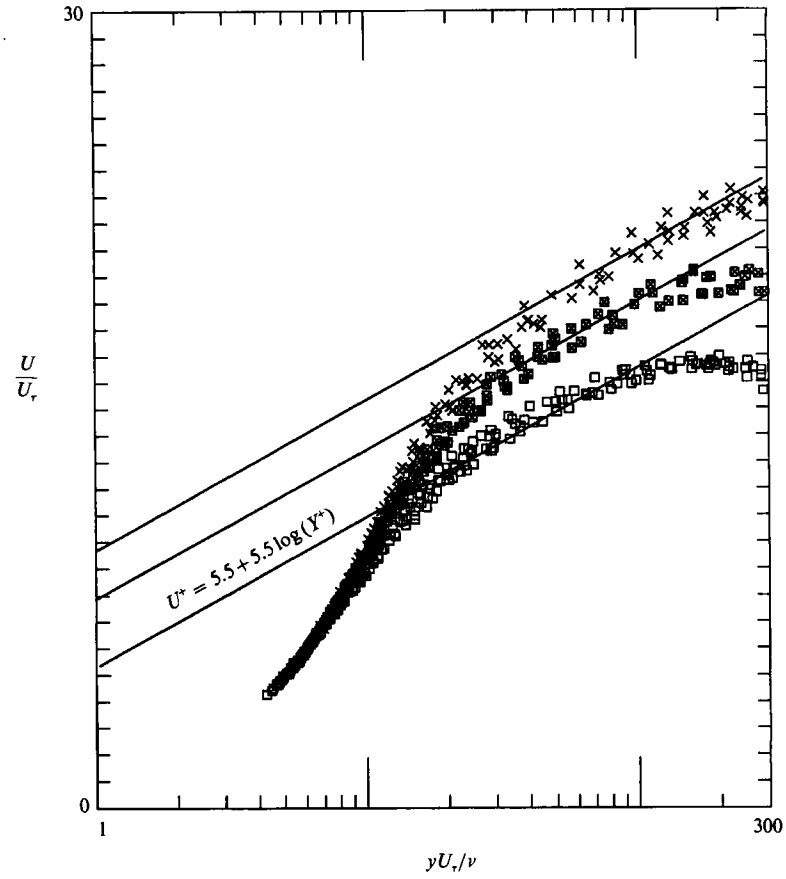

FIGURE 11. The velocity distribution near the wall plotted in wall coordinates. For symbols see table 1.

3.4. *The wall layer*

A semi-logarithmic plot of the mean velocity distribution in the wall region is shown in figure 11 for approximate Re_j values of 5000, 10000 and 19000. It is clear that the velocity profile near the surface is not universally represented in wall coordinates, as it is in the turbulent boundary layer. A logarithmic profile might be fitted to the data between $30 < U_\tau Y/\nu < 130$ for $Re_j = 5000$ and between $30 < U_\tau Y/\nu < 300$ for the highest Reynolds number. One may even fit a universal slope of 5.5 to all the curves shown in figure 11, but the intercept of the measured values of U/U_τ at $U_\tau Y/\nu = 1$ varies from approximately 5.5 to 9.5. The additive constant obtained in this way is consistent with the observations of Myers, Scahuer & Eustis (1963), Bradshaw & Gee (1962) and R. P. Patel (1962). However, all these authors also question the universality of the constant A in the equation $U/U_\tau = A\log(U_\tau Y/\nu)+B$ and they propose constants varying from 3.9 to 4.75. Ozarapoglu (1973) attributes the variation in both constants to corrections which should have been applied to the data acquired by both impact tubes and hot-wire probes. Since such corrections cannot be easily applied, because they require knowledge of v' fluctuation level very close to the wall, we checked the consistency of our results by resorting to the 'outer' scaling laws which are Reynolds-number independent at least in the range of Re_j considered.

We have shown (figure 7) that the normalized velocity profile measured at $Y \leqslant Y_m$ is dependent on Re_j. Taking a cue from observations made in a turbulent boundary

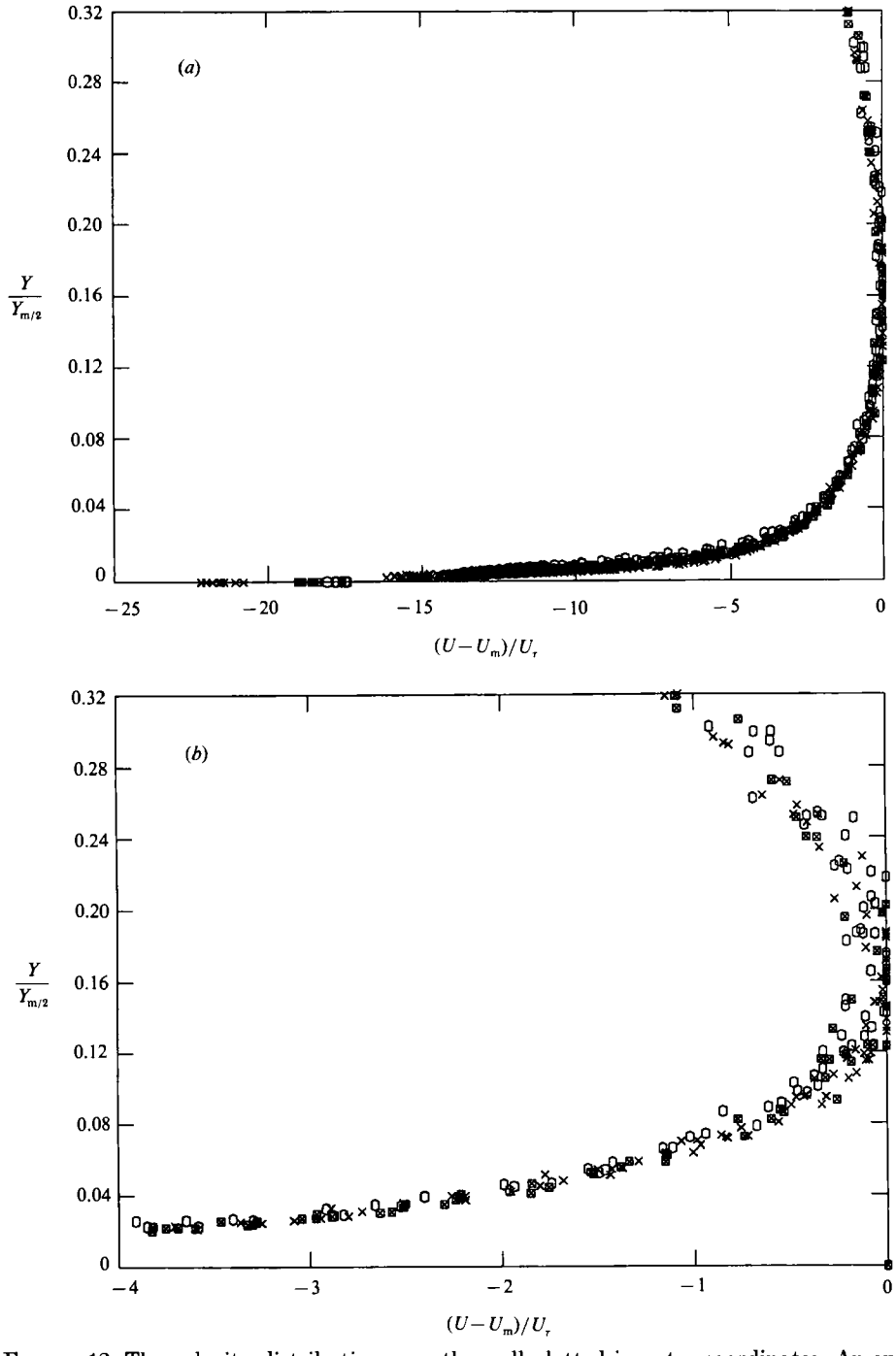

FIGURE 12. The velocity distribution near the wall plotted in outer coordinates. An enlargement of part of (*a*) is shown in (*b*). For symbols see table 1.

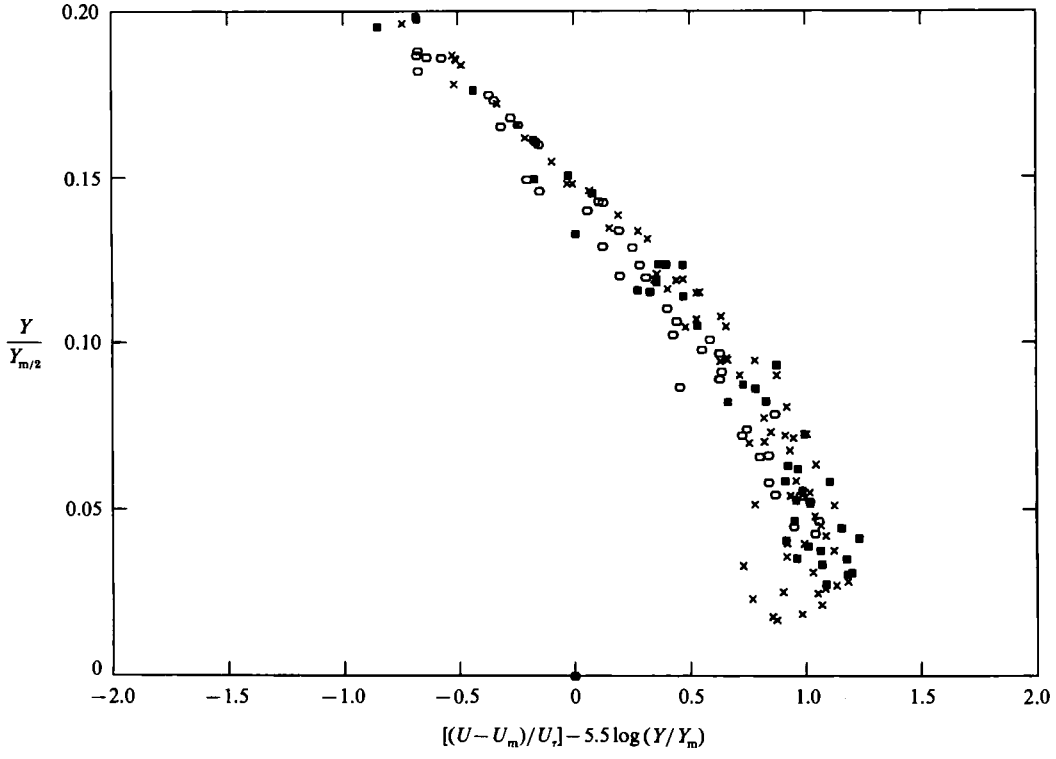

FIGURE 13. The velocity distribution near the wall plotted in outer coordinates and assuming the universality of the slope in the wall coordinates. For symbols see table 1.

layer (e.g. Coles & Hirst 1968), we shall assume that the flow might be universally self-similar were it expressed as

$$\frac{U}{U_\tau} = f\left(\frac{U_\tau Y}{\nu}\right) + A\Pi w\left(\frac{Y}{Y_m}\right). \tag{7}$$

If this correlation is allowed to extend to $Y = Y_m$ and $f(U_\tau Y/\nu) = A\log(U_\tau Y/\nu) + B$ then

$$\frac{U-U_m}{U_\tau} = A\log\left(\frac{Y}{Y_m}\right) + A\Pi\left[w\left(\frac{Y}{Y_m}\right) - w(1)\right], \tag{8}$$

where A is the 'universal constant' of the inner scaling law while B is eliminated. The reader should recall that the ratio $Y_m/Y_{m/2}$ is a constant and therefore the two lengthscales can be easily interchanged. A plot of $U-U_m/U_\tau$ *vs.* $Y/Y_{m/2}$ is shown in figure 12 for values of $Y/Y_{m/2} \leqslant 0.32$ and the results show a remarkable independence of Re_j even when the scale of the abscissa is greatly increased by limiting the experimental data shown to $U_\tau Y/\nu > 30$ (i.e. to the region where the logarithmic velocity distribution applies). We elected to plot the data shown in figure 12 up to $Y/Y_{m/2} = 0.32$ in order to show that the outer scaling law applies well beyond the location at which $U = U_m$ and certainly well beyond the location at which Reynolds stress vanishes, which occurs much closer to the solid surface.

Subtracting $5.5\log[Y/Y_m]$ from the previous results and replotting them in figure

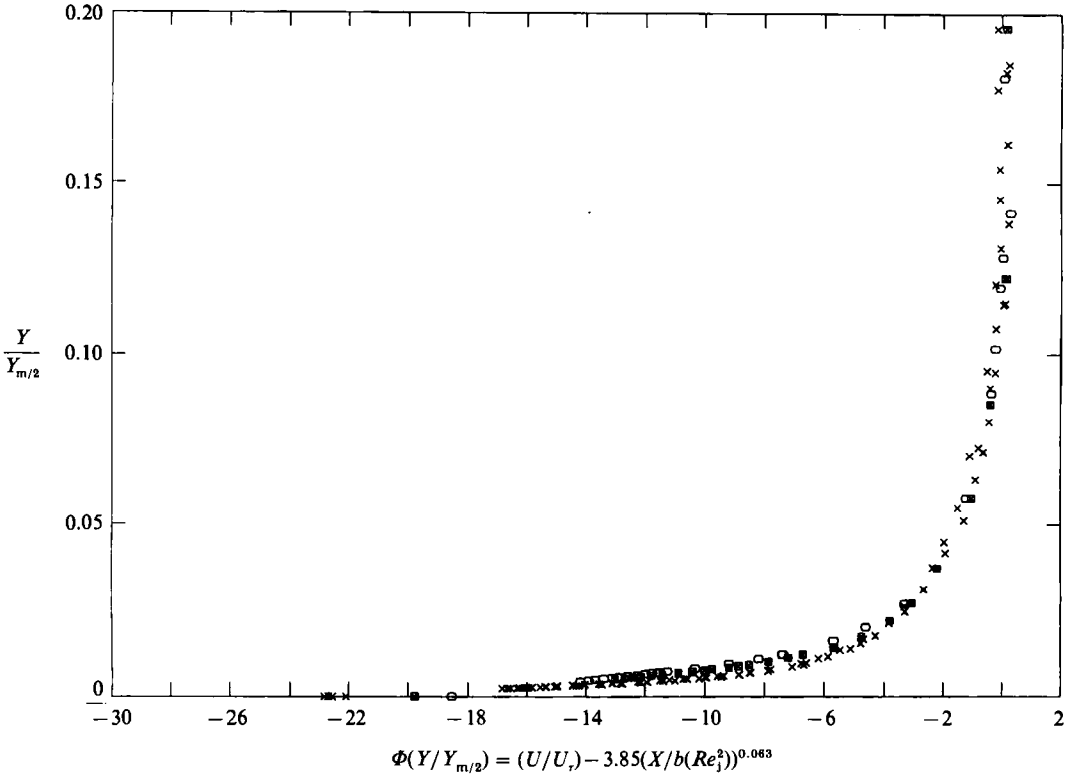

FIGURE 14. The applicability of the general similarity to the wall region. For symbols see table 1.

13 shows some deterioration in the similarity profile, suggesting that the constant A has some scatter around the nominal value of 5.5. The constant B may be calculated from every data point in the range of $30 < U_\tau Y/\nu < 130$ by subtracting from (8) the quantity $\{A \log(U_\tau Y/\nu) - [U_m/U_\tau]\}$.

One may also invoke the similarity considerations by using (4) and (5) to get

$$\frac{U_m}{U_\tau} = 3.85\xi^{0.063} \quad \text{or} \quad \frac{U}{U_\tau} - 3.85\xi^{0.063} = \Phi\left[\frac{Y}{Y_{m/2}}\right]. \tag{9}$$

The function Φ is plotted in figure 14 for three sets of data in which Re_j varied between 7500 and 19000. All the results collapse onto a single curve as expected from consistency considerations. One may use this result to calculate B again.

The dependence of B on ξ can be determined from the relation:

$$\frac{U_m}{U_\tau} = A \log\left(\frac{Y_m U_\tau}{\nu}\right) + B + A\Pi w(1) \tag{10}$$

because the variables U_m, Y_m and U_τ are all functions of ξ.

The calculated values of B were not constant but varied between 4.9 to 9.2, corresponding to $3700 \leqslant Re_j \leqslant 19300$. These values agree quite well with the intercepts with the ordinate of the straight lines drawn in figure 11.

4. Discussion and conclusions

The central core of a two-dimensional turbulent wall jet in a quiescent fluid is self-similar when it is scaled by the kinematic momentum flux at the nozzle and the viscosity of the fluid. The flow is independent of Re_j provided that the latter exceeds a certain threshold level. This scaling is very useful because it provides a convenient way to determine skin friction from the streamwise decrease of the momentum flux (equation (6)). The skin friction, which can be independently determined from the mean velocity gradient near the solid surface $\tau_w/\rho = \nu(\mathrm{d}U/\mathrm{d}Y)_w$, may also be expressed in terms of the self-similar velocity profile shown in figure 3 (i.e. $U = U_m f(Y/Y_{m/2})$ and when substituted into the momentum integral equation yields

$$-\kappa \frac{\mathrm{d}}{\mathrm{d}x}[U_m^2 Y_{m/2}] = \frac{\nu U_m}{Y_{m/2}} f'(0). \tag{11}$$

The significance of the proper scaling becomes evident when the dependence of U_m and $Y_{m/2}$ on X is substituted into (11). By choosing the conventional scaling

$$(U_m/U_j) = A_u(X/b)^n; \quad (Y_{m/2}/b) = A_y(X/b)^m$$

used in the literature one obtains

$$f'(0) \propto Re_j(X/b)^{2m+n-1}. \tag{12}$$

Choosing the scaling given in (3) gives

$$f'(0) \propto (\xi)^{2m+n-1}. \tag{13}$$

It is implausible that the skin friction far downstream of the nozzle will depend on Re_j, which can only influence the character of the flow within the nozzle and its vicinity. One may also observe from the momentum integral equation, that either scaling may be applied to the free jet. It is clear from figure 7 that the normalized velocity gradient near the wall is not self-similar, regardless of the type of scaling applied to U_m or $Y_{m/2}$. A complete self-similarity in a semi-bounded flow like the wall jet or a boundary layer cannot be anticipated because of the different scaling laws for the inner and the outer region. Nevertheless, the very weak dependence on X of the normalized velocity distribution near the surface may be attributed to the exponent of ξ (or of X/b) calculated above. This exponent is 0.18 when one accounts for the virtual origin of the flow.

The inner region of the wall jet between the solid surface and the location at which the velocity attains its local maximum may be scaled in an analogous fashion to a turbulent boundary layer. The 'defect law' which relates the difference between the local velocity and the velocity maximum $(U-U_m)$ to U_τ, Y and Y_m is valid throughout most of the region with the exception of the viscous sublayer. Dimensional considerations yield the following:

$$\frac{U-U_m}{U_\tau} = f\left(\frac{Y}{Y_m}\right) \propto f\left(\frac{Y}{Y_{m/2}}\right),$$

where $Y_{m/2}$ was used to replace Y_m since it is a constant multiple of Y_m.

On the other hand, in order to derive the logarithmic velocity distribution in the wall region it is sufficient to assume either: (i) that the total shear stress is constant and equivalent to the stress at the wall and (ii) that the changes in the local mean velocity are independent of viscosity; or by using the 'defect law' that changes in the

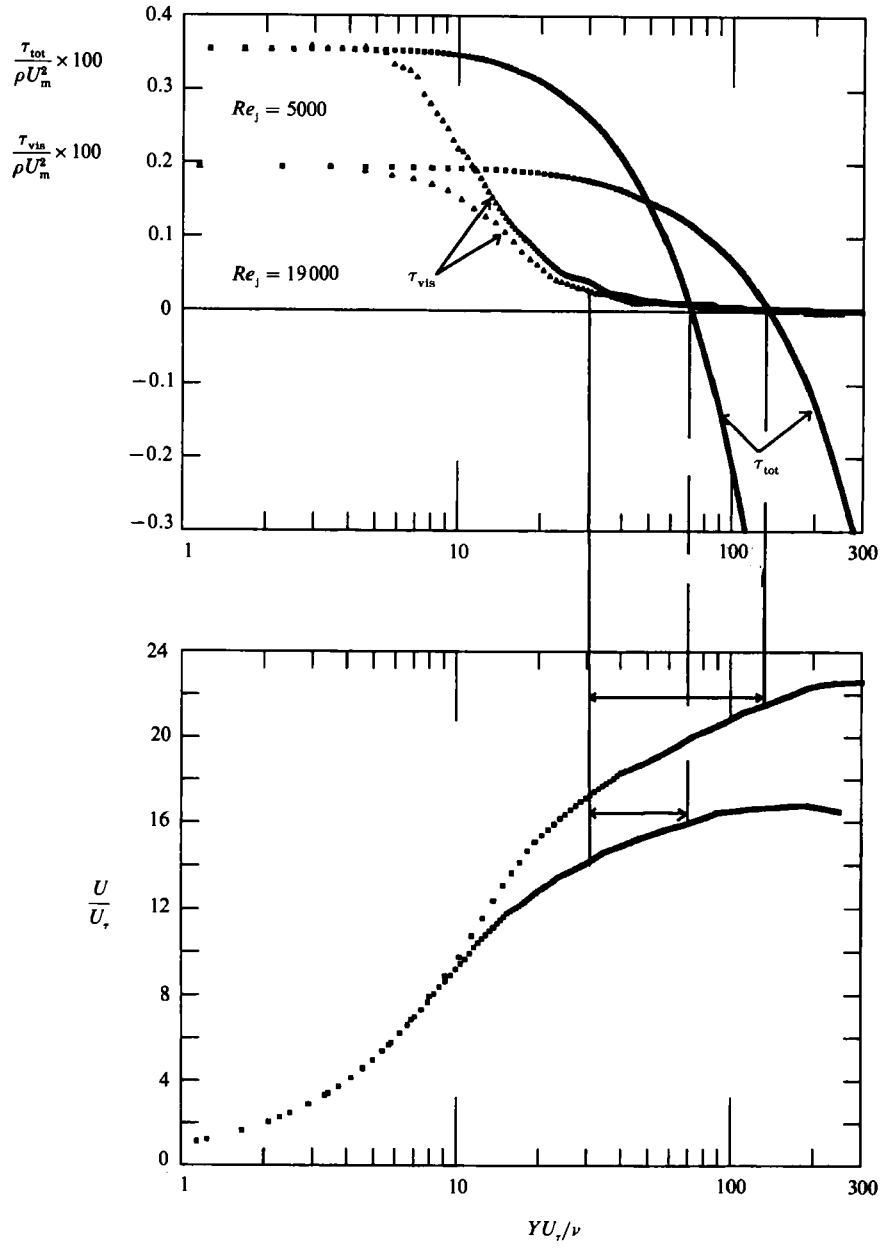

FIGURE 15. A comparison of the total and the viscous stress distributions near the surface plotted in wall coordinates.

local mean velocity occur so far from Y_m that they are independent of this dimension. All of these arguments were used to prove that an overlap exists between the region governed by the law of the wall and the region scaled by the outer law.

We computed the stress distribution by integrating the momentum equation from the wall outward, requiring the entire stress to be viscous at the wall. The results of these computations are plotted in figure 15 for $Re_j \approx 5000$ and 19000. The viscous stress vanishes at $U_\tau Y/\nu > 30$ as anticipated from data accumulated in turbulent boundary layers. However, the total stress is not constant at $U_\tau Y/\nu > 30$. In fact for

$Re_j \approx 5000$ the total stress starts decreasing at $YU_\tau/\nu > 8$ while for the higher Re_j it does so at > 30. The shear stress vanishes at the lower Reynolds number at $U_\tau Y/\nu \approx 60$ and at the higher Re_j at ≈ 120. Since the assumed existence of an inviscid constant stress layer did not materialize, one of the important assumptions used in deriving the logarithmic velocity distribution for the wall jet did not apply in the present case.

On the other hand, the derivation of the logarithmic velocity profile from the defect-law relation requires that the distance from Y_m to the logarithmic region will be much larger than the width of the logarithmic region itself. This assumption does not fit the present conditions either, since the distance from Y_m to the region where the logarithmic profile occurs is only 50 wall units at $Re_j = 5000$ and increases to approximately 100 wall units at the higher Reynolds numbers (figure 11). This is in sharp contrast to channel, pipe and boundary-layer flows, where the nominal thickness of the logarithmic region is an order of magnitude smaller than the thickness of the boundary layer or the radius of the pipe. The velocity defect law and the law of the wall may still apply to a wall jet provided that the Reynolds number is an order of magnitude higher than used in this experiment. One may possibly derive the logarithmic velocity distribution on the basis of other assumptions or models (e.g. Prandtl's mixing-length model) but their validity will have to be tested. Thus the equilibrium, to which we were so accustomed in the boundary layer, may not apply to the wall jet because the distance at which $U = U_m$ is so close to the surface that the importance of the inertia terms increases as rapidly with Y as the viscous term diminishes.

The intrusion of the outer scaling to the viscous sublayer might be associated with a rapid mixing process which takes place across the region where the velocity in the wall jet is maximum. Since this mixing process cannot stop at $Y = Y_m$, one may expect that the outer scaling law, as expressed in equation (8), will also apply at larger distances from the wall; and in fact the outer scaling may be applied up to $Y/Y_m \approx 4$ (or $Y/Y_{m/2} \approx 0.6$). This implies that there is a large region of overlap between the bulk parameters U_m and $Y_{m/2}$ which scale the core of the wall jet and the 'outer' (boundary-layer type) scaling laws. Consequently the restraining effects of the surface are felt far beyond $Y = Y_m$ in spite of the fact that the viscous effects are limited to $U_\tau Y/\nu < 30$.

The work was supported in part by a grant from AFOSR (contract number AFOSR-88-0176) and monitored by Dr J. McMichael. The authors also wish to thank Professor B. G. Newman for his help and advice and Professor D. Coles for his remarks.

REFERENCES

BRADSHAW, P. & GEE, M. Y. 1960 Turbulent wall jets with and without an external stream. *Aero. Res. Coun. R & M* 3252.

COLES, D. 1956 The law of the wake in a turbulent boundary layer. *J. Fluid Mech.* **1**, 191.

COLES, D. E. & HIRST, E. A. 1968 *AFOSR-IFP Stanford Conf. on Computation of Turbulent Boundary-Layers, Thermosciences Division, Stanford University.*

FORTHMANN, E. 1934 Uber turbulente Strahlausbreitung. *Ing. Arch.* **5**, 42.

GUITTON, D. E. & NEWMAN, B. G. 1977 Self-preserving turbulent wall jets over convex surfaces. *J. Fluid Mech.* **81**, 155.

IRWIN, H. P. A. H. 1973 Measurements in a self-preserving plane wall jet in a positive pressure gradient. *J. Fluid Mech.* **61**, 33.

LAUNDER, B. E. & RODI, W. 1981 The turbulent wall jets. *Prog. Aerospace Sci.* **19**, 81.

LAUNDER, B. E. & RODI, W. 1983 The turbulent wall jet – measurements and modeling. *Ann. Rev. Fluid Mech.* **15**, 429.

MYERS, G. E., SCAHUER, J. J. & EUSTIS, R. H. 1963 Plane turbulent wall jet flow development and friction factor. *Trans. ASME* J: *J. Basic Engng* **85**, 47.

NARASIMHA, R., NARAYAN, K. Y. & PARTHASARATHY, S. P. 1973 Parametric analysis of turbulent wall jets in still air. *Aeronaut. J.* **77**, 335.

NEWMAN, B. G. 1961 The deflexion of plane jets by adjacent boundaries – Coanda effect. In *Boundary Layer and Flow Control.* Pergamon.

OZARAPOGLU, V. 1973 Measurements in incompressible turbulent flows. D.Sc. thesis, Laval University, Quebec City.

PATEL, R. P. 1962 Self preserving two dimensional turbulent jets and wall jets in a moving stream. M.Sc. thesis, McGill University, Montreal.

PATEL, V. C. 1965 Calibration of the Preston tube and limitations on its use in pressure gradients. *J. Fluid Mech.* **23**, 185.

SCHWARZ, W. H. & COSART, W. P. 1961 The two-dimensional turbulent wall-jet. *J. Fluid Mech.* **10**, 481.

SIGALLA, A. 1958 Measurements of a skin friction in a plane turbulent wall jet. *J. R. Aero. Soc.* **62**, 873.

SREENIVASAN, K. R. & NARASIMHA, R. 1982 Equilibrium parameters for two-dimensional turbulent wakes. *Trans. ASME* I: *J. Fluids Engng* **104**, 167.

TAILLAND, A. & MATHIEU, J. 1967 Jet parietal. *J. Méc.* **6**, 1.

WILLS, J. A. B. 1962 The correction of hot-wire readings for proximity to a solid boundary. *J. Fluid Mech.* **12**, 388.